

1 **Relation between rich-club organization versus brain functions and functional recovery**  
2 **after acute ischemic stroke**

3

4 Lu Wang<sup>1</sup>, Kui Kai Lau<sup>3</sup>, Leonard SW Li<sup>3</sup>, Yuen Kwun Wong<sup>3</sup>, Christina Yau<sup>4</sup>, Henry KF Mak<sup>1,2</sup>, Edward S  
5 Hui<sup>1,2,\*</sup>

6 <sup>1</sup> Department of Diagnostic Radiology, University of Hong Kong, Pokfulam, HKSAR

7 <sup>2</sup> State Key Laboratory of Brain and Cognitive Sciences, University of Hong Kong, Pokfulam, HKSAR

8 <sup>3</sup> Department of Medicine, University of Hong Kong, Pokfulam, HKSAR

9 <sup>4</sup> Department of Occupational Therapy, Tung Wah Hospital, HKSAR

10 \* Corresponding author

11

12 **Data availability**

13 Available upon request.

14

15 **Funding**

16 This work was supported by the Research Grants Council of the Hong Kong Special Administrative Region,  
17 China, HKU 17108514.

18

19 **Conflict of interest**

20 None.

21

22 **Ethics approval**

23 This study was approved by the local Institutional Review Board

24

25 **Patient consent**

26 Informed consent was obtained from all patients.

27

28 **Permission to reproduce material from other sources**

29 Not applicable.

30

31 **Clinical trial registration**

32 Not applicable.

33

34

35 **Abstract**

36 Studies have shown that rich-club may underlie brain function and be associated with many  
37 brain disorders. In this study, we aimed to investigate the relation between poststroke brain  
38 functions and functional recovery versus the rich-club organization of the structural brain  
39 network of patients after first-time acute ischemic stroke. A cohort of 16 first-time acute  
40 ischemic stroke patients (11 males; 5 females) was recruited. Structural brain networks were  
41 measured using diffusion tensor imaging within 1 week and at 1, 3 and 6 months after stroke.  
42 Motor impairment was assessed using the Upper-Extremity Fugl-Meyer motor scale and  
43 activities of daily living using the Barthel Index at the same time points as MRI. The rich-club  
44 regions that were stable over the course of stroke recovery included the bilateral dorsolateral  
45 superior frontal gyri, right supplementary motor area, and left median cingulate and  
46 paracingulate gyri. The network properties that correlated with poststroke brain functions were  
47 mainly the ratio between communication cost ratio and density ratio of rich-club, feeder and  
48 local connections. The recovery of both motor functions and activities of daily living were  
49 correlated with higher normalized rich club coefficients and shorter length of local connections  
50 within a week after stroke. The communication cost ratio of feeder connections, the length of  
51 rich-club and local connections, and normalized rich club coefficients were found to be  
52 potential prognostic indicators of stroke recovery. Our results provide additional support to the  
53 notion that different types of network connections play different roles in brain functions as well  
54 as functional recovery.

55

## 56 **Introduction**

57 Approximately 80% of patients suffer from motor impairment after stroke.<sup>1,2</sup> Brain plasticity  
58 mechanisms, including activity-dependent rewiring and synapse strengthening, may likely  
59 underlie the recovery of brain functions.<sup>3-6</sup> Previous studies have investigated the relation  
60 between motor recovery after stroke and the structural connectivity of local pathways, such as  
61 corticospinal<sup>7-10</sup>, alternate corticofugal<sup>11,12</sup> and corticocortical pathways<sup>13,14</sup>. The relation  
62 between motor recovery and structural connectivity in stroke patients has also been  
63 investigated by large-scale analysis of structural connectivity<sup>15</sup>.

64 Neuroarchitecture can be understood not only at the local and global scales, as is usually  
65 performed, but also in specific groups of brain regions and the relationship among them, known  
66 as rich-club organization<sup>16</sup>. Rich-club organization is composed of brain regions that are  
67 closely connected, i.e., high centrality, and has been found to serve brain functions<sup>17</sup>. Rich-  
68 club organization may dominate the entire brain network<sup>18</sup>, and has been regarded as the core  
69 of communication of the whole human brain<sup>19</sup>. The brain regions that form rich-club  
70 organization in healthy adults are bilateral frontoparietal and subcortical regions, including the  
71 precuneus, superior frontal cortex, parietal cortex, putamen, hippocampus and thalamus.<sup>20</sup>  
72 Neurological diseases and disorders, such as, schizophrenia<sup>21</sup>, Huntington's disease<sup>22</sup>, multiple  
73 sclerosis<sup>23</sup>, traumatic brain injury<sup>24</sup>, and Alzheimer's disease<sup>25</sup>, have been shown to impair  
74 rich-club organization.

75 Two prior studies have investigated the relation between poststroke functional outcomes  
76 related to motor function and rich-club metrics, such as the number of rich-club nodes affected  
77 by stroke<sup>26</sup>, and path length and the average distance between regions<sup>27</sup>. Considering that there  
78 is a lack of understanding of the longitudinal changes in rich-club organization after stroke,  
79 and the relation between rich-club organization versus poststroke brain functions and  
80 functional recovery, we therefore aimed to investigate whether rich-club organization would  
81 change over the course of stroke recovery, association between network metrics and poststroke  
82 brain functions, and the network metrics that may predict functional recovery.

## 83 **Materials and methods**

### 84 **Subjects and functional assessments**

85 Stroke patients (n = 16; 11 male; mean age 65.8 ± 11.0; infarct side: 50% left) with first-time  
86 acute ischemic stroke were recruited between September 2015 and July 2018 with informed  
87 consent. MRI and functional assessments were performed within 1 week (n = 12) and at 1 (n =

88 16), 3 (n = 13) and 6 (n = 9) months after acute ischemic stroke. Functional assessments  
89 included the Upper-Extremity Fugl-Meyer motor scale (UE-FM) and Barthel index (BI). The  
90 UE-FM was developed to quantitatively assess the severity of motor impairment of the upper  
91 extremity due to hemiplegic stroke and is based on the well-defined stages of motor recovery<sup>28</sup>.  
92 The BI was developed to quantitatively assess disability and functional outcomes<sup>29</sup>. All patients  
93 received rehabilitation at the Acute Stroke Unit of Queen Mary Hospital after admission due  
94 to acute stroke. After an average of 5 days after admission, patients were transferred to the  
95 Stroke Rehabilitation Ward of Tung Wah Hospital for more intensive rehabilitation. All  
96 patients underwent conventional occupational rehabilitation therapy sessions, including  
97 activities of daily living training, upper limb functional training, cognitive perceptual training  
98 and functional task training. All procedures were carried out following the operational  
99 guidelines of the Human Research Ethics Committee, and all protocols were approved by the  
100 Institutional Review Board of the University of Hong Kong/Hospital Authority Hong Kong  
101 West Cluster.

## 102 **Image acquisition**

103 All MRI scans were performed using a 3.0 T MRI scanner (Achieva TX, Philips Healthcare,  
104 Best, The Netherlands) with a body coil for excitation and an 8-channel head coil for reception.  
105 Diffusion tensor imaging (DTI) was performed using single-shot spin-echo echo planar  
106 imaging, consisting of non-diffusion-weighted images (b0) and diffusion-weighted images  
107 (DWIs) with b-values of 1000 s/mm<sup>2</sup> along 32 gradient directions, with the following  
108 parameters: TR/TE = 4000/81 ms, field-of-view = 230 × 230 mm<sup>2</sup>, reconstructed  
109 resolution = 3 × 3 mm<sup>2</sup>, 33 contiguous slices with thickness of 3 mm, SENSE factor = 2,  
110 number of averaging = 2, total scan time ≈ 5 minutes. TI-weighted image were acquired using  
111 3D magnetization prepared-rapid gradient echo (MPRAGE) with the following parameters:  
112 TR/TE/TI = 7/3.17/800 ms, field-of-view = 240 × 240 mm<sup>2</sup>, reconstruction resolution = 1 ×  
113 1 × 1 mm<sup>3</sup>, 160 contiguous slices, scan time ≈ 6 min.

## 114 **Image pre-processing**

115 All of the pre-processing procedures were performed using SPM12  
116 (<https://www.fil.ion.ucl.ac.uk/spm/>). Head motion correction was performed by registering  
117 DWIs to b0 images<sup>30</sup>. MPRAGE images were first reoriented taking the anterior commissure<sup>31</sup>  
118 as the origin. The reoriented MPRAGE images were normalized to the MNI152 template to  
119 obtain a transformation matrix *M*. The MNI152 template was then inversely normalized to

120 MPRAGE images by the inverse of  $M$ ,  $M^{-1}$ . The inverse normalized MNI152 template was  
121 non-linearly registered to DWIs, and a transformation matrix  $T$  was obtained. In this way, an  
122 inverse warping transformation from the standard space to the native DTI space was obtained.

### 123 **Network construction**

124 Tractography: Diffusion tensor and diffusion metrics were obtained using the Diffusion  
125 Toolkit<sup>32</sup>. White matter tractography was obtained using TrackVis (<http://trackvis.org>) using  
126 Fibre Assignment by Continuous Tracking (FACT)<sup>33,34</sup> with an angle threshold of  $45^\circ$  and  
127 random seed of 32. Spine filter was used to smooth the fibre tracks.

128 Network node definition: The Automated Anatomical Labelling 2 (AAL2) atlas<sup>35</sup> in the  
129 standard space was inversely wrapped to the individual DTI native space according to  $M^{-1}$   
130 and  $T$ . Ninety-four cortical regions (47 in each hemisphere) were obtained, and each region  
131 was regarded as a node. Of these, 10 regions were excluded, namely, the left and right inferior  
132 occipital gyrus, left and right fusiform gyrus, left and right superior temporal pole, left and  
133 right middle temporal pole and left and right inferior temporal pole, due to variations in brain  
134 coverage.

135 Network link definition: The UCLA Multimodal Connectivity package was used to calculate  
136 the number and length of fibres between each pair of regions. Two regions were considered as  
137 connected when a fibre connected them. The link weight was defined as the fibre count between  
138 two regions.

### 139 **Network topology metrics**

140 MATLAB (2018b) and the Brain Connectivity Toolbox  
141 (<https://sites.google.com/site/bctnet/>)<sup>36</sup> were used to calculate brain network topology metrics.  
142 The metrics included (1) node degree, the number of nodes that a given node is connected to;  
143 (2) node strength, the sum of the weight of connected links of a node; (3) local clustering  
144 coefficient, the connection properties within the neighbourhood of a node; (4) global efficiency,  
145 the average inverse shortest path length in the network; (5) local efficiency, the global  
146 efficiency computed on node neighbourhoods; and (6) node betweenness centrality, the  
147 fraction of all shortest paths in the network that contain the node of interest.

### 148 **Rich-club organization**

149 R (3.6.0) was used to estimate rich-club organization for each subject at each time point using  
150 a previously published method<sup>37</sup>. The weighted rich-club coefficient was calculated in 4 steps.  
151 First, for each node degree ( $k$ ), a subnetwork was obtained by extracting the nodes with degree  
152 greater than  $k$  and the links among them. Second, for each subnetwork, the total number of  
153 links ( $n$ ) and the sum of weights of the links ( $W$ ) were calculated. Third, the  $n$  largest weights  
154 of the whole network were summed. Finally, the weighted rich-club coefficient of this  
155 subnetwork was subsequently calculated as follows:<sup>38</sup>

$$156 \quad \varphi^w(k) = \frac{W_{>k}}{\sum_{l=1}^n w_l^{\text{ranked}}}$$

157 where  $W_{>k}$  represents total weights of the links of nodes with degree larger than  $k$ , and  
158  $\sum_{l=1}^n w_l^{\text{ranked}}$  the sum of the  $n$  largest weights of the links. However, nodes with lower degree  
159 in a network have lower possibilities of sharing links with each other by coincidence, and even  
160 random networks generate increasing rich-club coefficients as a function of increasing degree  
161 threshold  $k$ . To circumvent this effect, 1,0000 random networks with the same size and same  
162 degree distribution of the network of interest were generated. The average of the rich-club  
163 coefficients of the 1,0000 random networks were calculated,  $\varphi_{\text{random}}$ . The normalized rich-  
164 club coefficient of the network of interest was defined as follows:<sup>16,37</sup>

$$165 \quad \varphi_{\text{norm}} = \frac{\varphi_k}{\varphi_{\text{random}}}$$

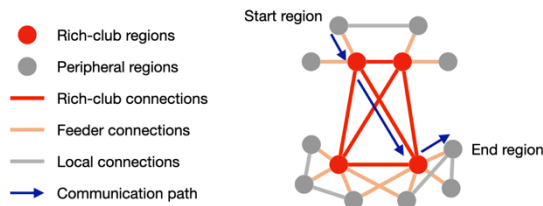
166 A subnetwork is considered a rich-club organization when  $\varphi_{\text{norm}}(k) > 1$ .<sup>21,39</sup>

167 A node can be evaluated as a rich-club node when  $k = \{k_1, k_2, \dots, k_n\}$ , in which the highest  $k$   
168 was called the highest rich-club level. Each node of a rich-club organization was given a score  
169 according to their highest rich-club level. Then, after averaging the score of nodes from all  
170 participants at the same time point after stroke, the top 8 nodes (i.e., 10% of all nodes) were  
171 selected as rich-club nodes.

## 172 **Node and connection types**

173 There are two types of nodes in a brain network, namely, rich-club nodes and peripheral nodes.  
174 Furthermore, there are three types of connections in a rich-club organization (**Figure 1**),  
175 namely, rich-club connections (between rich-club nodes), feeder connections (between rich-  
176 club nodes and non-rich-club nodes), and local connections (between non-rich-club nodes).<sup>19</sup>

177



178 **Figure 1** Illustration of different node and connection types. A communication path was  
179 indicated by blue arrows.

## 180 Network communication

181 The cost of a link was defined as the product between its length and density (the count of  
182 streamlines between two brain regions). Communication cost was defined as the product  
183 between length and density based on their topological distance<sup>19</sup>. To calculate the  
184 communication cost of the three kinds of connections in a rich-club organization, first, the  
185 shortest paths between 84 nodes were calculated. Then, each link of the shortest paths was  
186 divided into three categories (rich-club, feeder and local connections). Next, the  
187 communication cost of each link was calculated by multiplying its length and density. Finally,  
188 the communication cost of three kinds of connections was obtained by summing the  
189 communication cost for links of each kind. The metric ratio of a connection type was defined  
190 as the sum of metrics of this connection type divided by the total metric of the whole network.  
191 For example, density ratio of feeder connections was defined as total density of feeder  
192 connections divided by total density of all connections. The communication cost/density ratio  
193 was defined as the communication cost ratio divided by the density ratio, which was the weight  
194 of brain communication capacity<sup>19</sup>.

## 195 Statistical analysis

196 Statistical analyses were performed by R (version 3.6.0) with the functions lmer ([https://cran.r-](https://cran.r-project.org/web/packages/lme4/lme4.pdf)  
197 [project.org/web/packages/lme4/lme4.pdf](https://cran.r-project.org/web/packages/lme4/lme4.pdf)) and blmer ([https://cran.rproject.org/web/packages](https://cran.rproject.org/web/packages/blme/blme.pdf)  
198 [/blme/blme.pdf](https://cran.rproject.org/web/packages/blme/blme.pdf)). To simplify the statistical analyses on the local structural brain networks, the  
199 left and right hemispheres were flipped so that the left hemisphere always corresponded to the  
200 ipsilesional hemisphere. Due to attrition, some of the behavioural data and imaging data were  
201 not obtained. Imputation was thus performed on the behavioural data to increase the effective  
202 sample size for subsequent statistical analyses of prediction model. For patients no. 2, 13 and  
203 15, the behavioural data at 6 months after stroke were imputed from those at 3 months. Since  
204 patient nos. 11 and 16 had already made full recovery at the last follow-up, full behavioural

205 scores were assumed for the missing time points. After imputation, the 10 patients had  
 206 behavioural data for all 4 time points. The imputed behavioural data are underlined in **Table 1**.  
 207 To handle data with an unequal number of longitudinal measures, a Bayesian linear mixed  
 208 model<sup>40,41</sup> was used as the main model in the current study so that a posteriori estimation could  
 209 be maximized in a Bayesian setting. When necessary, linear mixed models were followed by  
 210 post hoc tests with Bonferroni corrections for multiple comparisons at  $p < 0.05$ . This study  
 211 mainly investigated three aspects: (1) to test whether functional assessments and network  
 212 metrics changed with time. Models were established with the functional assessments and  
 213 network metrics as responses, time as fixed variable, each subject as random variable, and age  
 214 and gender as covariates. (2) To test the correlations between network metrics and functional  
 215 assessments, models were established with the functional assessment data as responses,  
 216 network metrics as fixed variables, each subject as random variable, and age and gender as  
 217 covariates. (3) To identify biomarkers that may predict poststroke functional recovery, models  
 218 were established with poststroke functional recovery (change in functional assessment from  
 219 baseline) as responses, each subject as random variable, metrics at baseline as fixed variables,  
 220 and time, age and gender as covariates. After selecting the metrics that may be predictors of  
 221 responses, a linear mixed regression model was established by the stepwise method. In the  
 222 whole study, a best fitting model was chosen by comparing models using the likelihood ratio  
 223 test with the principle that the smaller the AIC was, the better the model was<sup>42</sup>. Additionally,  
 224 the simpler model was chosen when the gap in AIC values and likelihood ratio test results was  
 225 small.

226 **Table 1.** The baseline demographics and assessment of motor impairment (Upper-Extremity  
 227 Fugl-Meyer motor scale) and performance in activities of daily living (Barthel Index) of  $n =$   
 228 16 patients.

Patient	Side of lesion*	Upper-Extremity Fugl-Meyer Motor Scale (0–66)				Barthel Index (0–100)			
		< 1 week	1 month	3 months	6 months	< 1 week	1 month	3 months	6 months
		1	R	33	64	66	66	55	90
2	L	N.A.	63	63	<u>63</u>	N.A.	95	100	<u>100</u>
3	L	N.A.	5	14	18	N.A.	65	85	100
4	R	0	2	N.A.	N.A.	0	40	N.A.	N.A.
5	L	N.A.	31	40	49	N.A.	65	80	85
6	R	N.A.	48	62	63	N.A.	25	75	95
7	L	0	7	13	20	35	40	45	70
8	R	0	5	5	5	30	50	50	50
9	L	56	64	66	66	55	60	100	100
10	L	54	59	64	64	55	85	95	100

11	R	60	66	66	<u>66</u>	65	100	100	<u>100</u>
12	L	0	3	30	45	45	30	75	90
13	L	0	60	66	<u>66</u>	0	70	95	<u>95</u>
14	R	2	33	N.A.	N.A.	30	40	N.A.	N.A.
15	R	0	4	4	<u>4</u>	0	50	60	<u>60</u>
16	R	64	66	<u>66</u>	<u>66</u>	80	100	<u>100</u>	<u>100</u>

229 R: right; L: left; N.A.: not available

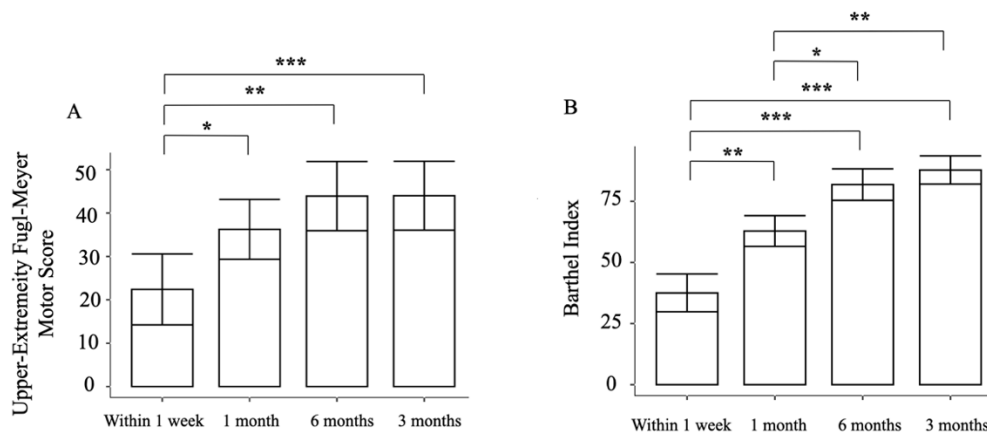
230 \*Left hemisphere was assigned as the ipsilesional hemisphere and right contralesional hemisphere.

231 Note that functional assessments that were underlined were obtained from data imputation.

## 232 Results

### 233 Patient demographics

234 MRI and functional assessments were performed on 12, 16, 13 and 9 patients within 1 week  
 235 and at 1, 3 and 6 months after first-time acute ischemic stroke, respectively, as shown in **Figure**  
 236 **2**. A linear mixed model was used to test the fixed effect of time on functional assessments.  
 237 UE-FM ( $\beta_{time} = 3.47$ ;  $\chi_1^2 = 13.68$ ,  $p < 0.001$ ) and BI ( $\beta_{time} = 7.94$ ,  $\chi_1^2 = 28.31$ ,  $p < 0.001$ )  
 238 significantly increased with time. Post hoc tests showed that UE-FM scores at 1 ( $p = 0.01$ ), 3  
 239 ( $p < 0.001$ ) and 6 ( $p < 0.001$ ) months were significantly higher than those within 1 week after  
 240 stroke. BI scores at 1, 3 and 6 ( $p < 0.001$ , all) months were significantly higher than those  
 241 within 1 week after stroke, and BI scores at 3 and 6 ( $p < 0.001$ , all) months were significantly  
 242 higher than 1 month after stroke.

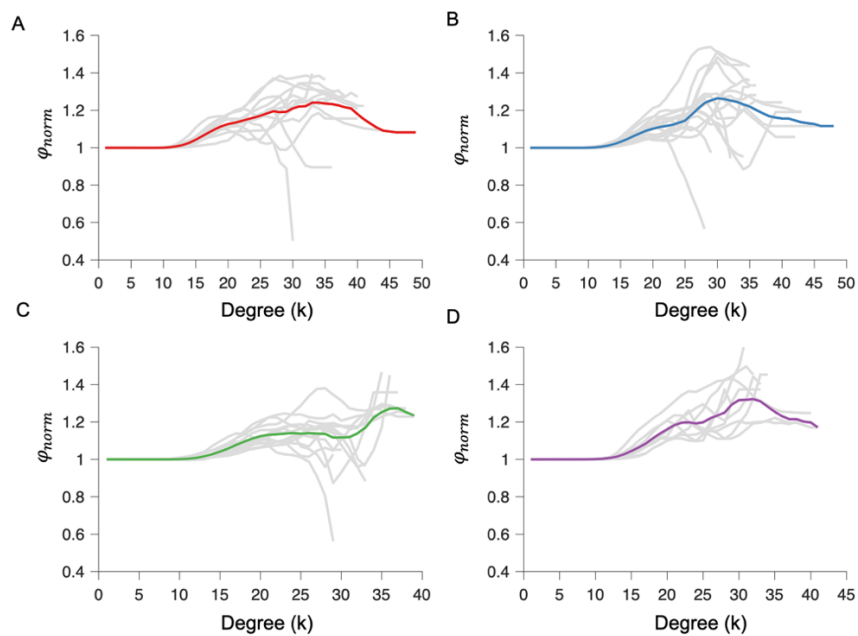


243

244 **Figure 2.** Bar chart with error bars (standard deviations) of the (A) Upper-Extremity Fugl-  
 245 Meyer motor scale and (B) Barthel index scores within 1 week ( $n = 12$ ), and at 1 ( $n = 16$ ), 3 ( $n$   
 246  $= 13$ ) and 6 ( $n = 9$ ) months after first-time acute ischemic stroke. Post hoc tests with Bonferroni  
 247 corrections for multiple comparisons across different time points were performed (\* $p < 0.05$ ,  
 248 \*\* $p < 0.01$ , \*\*\* $p < 0.001$ ).

## 249 Rich-club organizational changes after stroke

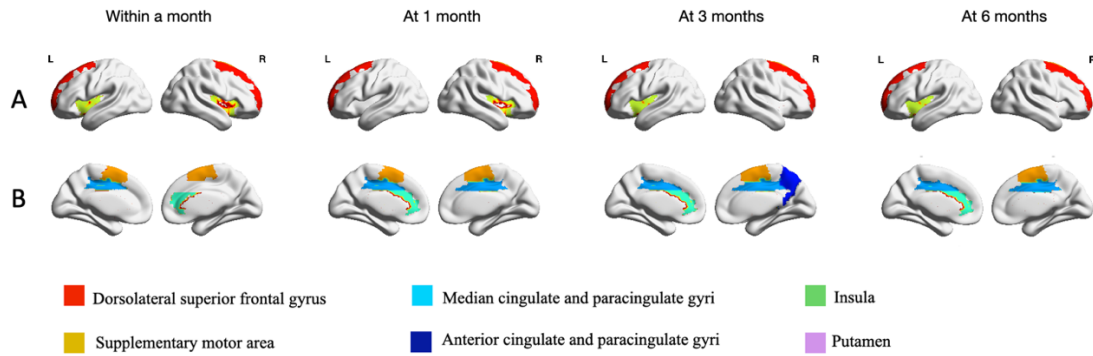
250 Rich-club organization was found from the structural brain network of patients within 1 week,  
251 and at 1, 3 and 6 months after first-time acute ischemic stroke (**Figure 3**). Not every patient  
252 (grey lines) had a normalized rich-club coefficient larger than 1 except at 6 months after stroke.  
253 Linear mixed model was used to test the effect of time after stroke on normalized rich-club  
254 coefficients with age and gender as covariates. Significant time effect on the normalized rich-  
255 club coefficients at  $k = 20$  ( $\chi_1^2 = 6.39$ ,  $p = 0.011$ ,  $\beta_{time} = 0.16$ ),  $21$  ( $\chi_1^2 = 5.89$ ,  $p = 0.015$ ,  
256  $\beta_{time} = 0.15$ ),  $k = 22$  ( $\chi_1^2 = 5.92$ ,  $p = 0.015$ ,  $\beta_{time} = 0.16$ ), and  $k = 23$  ( $\chi_1^2 = 6.02$ ,  $p = 0.014$ ,  
257  $\beta_{time} = 0.16$ ) were observed. The brain regions that were rich-club regions at each time point  
258 after stroke were listed in **Table 2** and shown in **Figure 4**. Notice that bilateral dorsolateral  
259 superior frontal gyrus, right supplementary motor area, and left median cingulate and  
260 paracingulate gyri remained as rich-club regions at all 4 time points.



261

262 **Figure 3.** Normalized rich-club coefficient of the structural brain network of patient within (A)  
263 1 week and at (B) 1, (C) 3 and (D) 6 months after first-time acute ischemic stroke. Grey lines:  
264 individual patient; Colored lines: average of all patients.

265



266

267 **Figure 4.** Rich-club regions at each time point after first-time acute ischemic stroke.

268 **Table 2** Rich-club regions at each time point after first-time acute ischemic stroke.

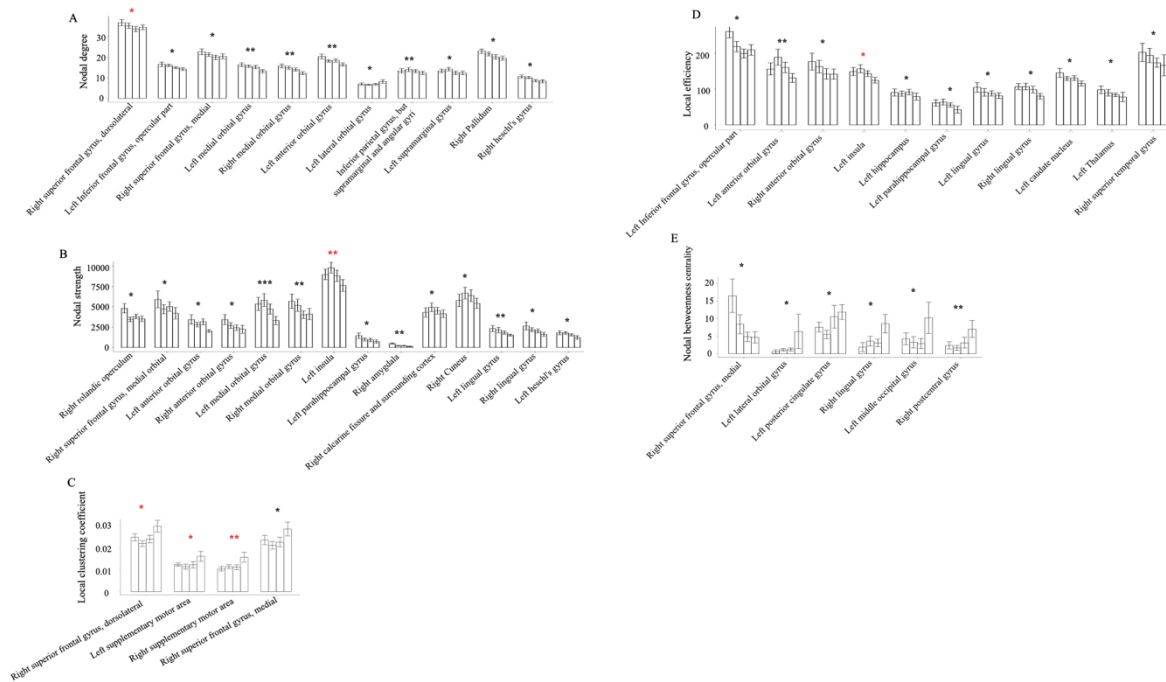
Rich-club regions	Side*	Time after acute ischemic stroke			
		< 1 week	1 month	3 months	6 months
Dorsolateral superior frontal gyrus	Left	√	√	√	√
	Right	√	√	√	√
Supplementary motor area	Left	√	√		
	Right	√	√	√	√
Insular	Left	√		√	√
	Right	√	√		
Anterior cingulate and paracingulate gyri	Left		√	√	√
	Right	√			
Median cingulate and paracingulate gyri	Left	√	√	√	√
	Right		√	√	√
Precuneus	Right			√	
Putamen	Left				√

269 \*Left hemisphere was assigned as the ipsilesional hemisphere and right contralesional hemisphere.

## 270 Longitudinal changes in network metrics after first-time acute ischemic stroke

271 The structural brain networks at local and rich-club scales over the course of stroke recovery  
 272 were examined. Metrics of the network at local scale pertain to the network metrics of each  
 273 brain region; rich-club scale to the mean link metrics of rich-club, feeder and local connections.  
 274 A linear mixed model was used to test the fixed effect of time after stroke on these network  
 275 metrics with age and gender as covariates, and subject as random variable. For the local scale,  
 276 the node degree, node strength, local clustering coefficient, local efficiency and nodal  
 277 betweenness centrality of a number of nodes changed with time after stroke (**Figure 5**). For  
 278 the rich-club scale (**Table 3**), significant negative time effect on the length of feeder

279 connections ( $\beta_{time} = -0.13, \chi_1^2 = 5.38, p = 0.020$ ) and communication cost ratio/density  
 280 ratio of local connections ( $\beta_{time} = -0.16, \chi_1^2 = 7.23, p = 0.007$ ) were observed. Significant  
 281 positive time effect on the density ratio of rich club connections ( $\beta_{time} = 0.15, \chi_1^2 = 5.10, p =$   
 282  $0.024$ ) and communication cost ratio/density ratio of feeder connections ( $\beta_{time} = 0.13, \chi_1^2 =$   
 283  $3.89, p = 0.049$ ) were observed.



284  
 285 **Figure 5.** The effect of time after first-time acute ischemic stroke on the metrics of brain  
 286 network at local scale: (A) node degree, (B) node strength, (C) local clustering coefficient, (D)  
 287 local efficiency and (E) nodal betweenness centrality. Only regions showing statistical  
 288 significance were displayed. \* $p < 0.05$ , \*\* $p < 0.01$ , \*\*\* $p < 0.001$ . Rich-club regions were  
 289 annotated with a red \*.

290 **Table 3.** The effect of time after first-time acute ischemic stroke on the metrics of brain  
 291 network at rich-club scale. Only metrics showing statistical significance were shown.

Connection Type	Network metric	$\beta_0$	$\beta_{time}$	$\chi^2$	Df	Pr ( $> \chi^2$ )
<b>Rich-club</b>	Density ratio	0.18	0.15	5.10	1	0.024
	Length	0.06	-0.13	5.38	1	0.020
<b>Feeder</b>	Communication cost ratio/density ratio	-1.30	0.13	3.89	1	0.049
<b>Local</b>	Communication cost ratio/density ratio	2.60	-0.16	7.23	1	0.007

292  $\beta_0$  and  $\beta_{\text{time}}$  are the fixed effects coefficients:  $\beta_0$  is the intercept,  $\beta_{\text{time}}$  is the linear slope; Df: degrees of freedom  
293 for the chi-square test.

## 294 **Relation between poststroke brain functions and network metrics**

295 A linear mixed model was used to test the relation between functional assessments and the  
296 metrics of brain network at rich-club scale with age and gender as covariates, and subject as  
297 random variable. The length ( $\beta_1 = -6.09, \chi_1^2 = 4.55, p = 0.033$ ) and cost ( $\beta_1 = -6.77, \chi_1^2 =$   
298  $4.34, p = 0.037$ ) of feeder connections, and the communication cost ratio/density ratio of rich  
299 club connections ( $\beta_1 = 4.54, \chi_1^2 = 4.25, p = 0.039$ ) were correlated with UE-FM. The  
300 communication cost ratio/density ratio of local ( $\beta_1 = -10.05, \chi_1^2 = 7.42, p = 0.006$ ), feeder  
301 ( $\beta_1 = 7.47, \chi_1^2 = 4.86, p = 0.028$ ), rich-club connections ( $\beta_1 = 11.60, \chi_1^2 = 11.66, p =$   
302  $0.001$ ), and the density ratio of rich-club connections ( $\beta_1 = 9.24, \chi_1^2 = 6.91, p = 0.009$ ) were  
303 correlated with BI. All statistical results were summarized in **Table 4**.

304 **Table 4.** Correlation between poststroke brain functions versus rich-club metrics.

Poststroke brain functions	Node/Connection type	Network metric	$\beta_0$	$\beta_1$	$\chi^2$	Df	Pr ( $> \chi^2$ )
UE-FM	Feeder connections	Cost	67.83	-6.77	4.34	1	0.037
		Length	78.69	-6.09	4.55	1	0.033
	Rich-club connections	Communication cost ratio/density ratio	85.82	4.54	4.25	1	0.039
BI	Feeder connections	Communication cost ratio/density ratio	163.76	7.47	4.86	1	0.028
	Local connections	Communication cost ratio/density ratio	178.83	-10.05	7.42	1	0.006
	Rich-club connections	Communication cost ratio/density ratio	172.24	11.60	11.66	1	0.001
		Density ratio	151.82	9.24	6.91	1	0.009

305 UE-FM: upper-extremity Fugl-Meyer motor scale; BI: Barthel index.

## 306 **Prediction of poststroke functional recovery using metrics of brain network at rich-club scale**

308 Linear mixed models were used to investigate the relation between changes in poststroke brain  
309 functions from baseline (i.e., poststroke functional recovery) and baseline metrics of brain  
310 network at rich-club scale as well as normalized rich-club coefficient. For the change in UE-  
311 FM, the length of rich-club connections ( $\beta_1 = 8.42, \chi_1^2 = 4.33, p = 0.037$ ), normalized rich-  
312 club coefficients at  $k = 19$  ( $\beta_1 = 14.06, \chi_1^2 = 7.05, p = 0.008$ ),  $k = 20$  ( $\beta_1 = 11.06, \chi_1^2 =$   
313  $6.05, p = 0.014$ ), the density ratio ( $\beta_1 = 9.49, \chi_1^2 = 5.07, p = 0.024$ ), cost ratio ( $\beta_1 =$

314 9.29,  $\chi_1^2 = 4.88, p = 0.027$ ), communication cost ratio ( $\beta_1 = 21.59, \chi_1^2 = 6.87, p = 0.009$ )  
 315 of feeder connections, and the length ( $\beta_1 = -12.96, \chi_1^2 = 5.13, p = 0.024$ ), density ratio  
 316 ( $\beta_1 = -8.94, \chi_1^2 = 4.75, p = 0.029$ ), cost ratio ( $\beta_1 = -9.50, \chi_1^2 = 5.53, p = 0.015$ ) and  
 317 communication cost ratio/density ratio ( $\beta_1 = -12.42, \chi_1^2 = 4.39, p = 0.036$ ) of local  
 318 connections were significantly correlated. For the change in BI, the density ( $\beta_1 =$   
 319  $-12.62, \chi_1^2 = 5.13, p = 0.024$ ), length ( $\beta_1 = -12.74, \chi_1^2 = 3.87, p = 0.049$ ) and cost ( $\beta_1 =$   
 320  $-13.18, \chi_1^2 = 5.92, p = 0.015$ ) of local connections, and normalized rich-club coefficients  
 321 were significantly correlated. These results were summarized in **Table 5**.  
 322 The network metrics that were selected to predict poststroke functional recovery were shown  
 323 in **Table 6**. The communication cost ratio of feeder connections, length of rich-club and local  
 324 connections, and normalized rich-club coefficient ( $k = 19$ ) could predict UE-FM changes  
 325 ( $\chi_4^2 = 23.33, p < 0.001$ ). The length of local connections and normalized rich-club coefficients  
 326 ( $k = 18, 19$ ) could predict BI changes ( $\chi_2^2 = 21.60, p < 0.001$ ).

327 **Table 5.** Correlation between poststroke functional recovery versus metrics of brain network  
 328 at rich-club scale.

Poststroke functional recovery*		Node/Connection type	Metric	$\beta_0$	$\beta_1$	$\chi^2$	Df	Pr ( $> \chi^2$ )
Change in UE-FM	Local connections		Length	-137.87	-12.96	5.13	1	0.024
			Density ratio	-88.68	-8.94	4.75	1	0.029
			Cost ratio	-84.21	-9.50	5.53	1	0.019
			Communication cost ratio/density ratio	4.42	-12.42	4.39	1	0.036
	Feeder connections		Density ratio	-89.45	9.49	5.07	1	0.024
			Cost ratio	-90.18	9.29	4.88	1	0.027
			Communication cost ratio	72.37	21.59	6.87	1	0.009
	Rich-club connections		Length	-80.29	8.42	4.33	1	0.037
		Rich-club		$\emptyset_{norm}$ ( $k = 19$ )	-131.33	14.06	7.05	1
			$\emptyset_{norm}$ ( $k = 20$ )	-109.59	11.06	6.05	1	0.014
Change in BI	Local connections		Density	-93.51	-12.62	5.13	1	0.024
			Length	-89.66	-12.74	3.87	1	0.049
			Cost	-94.48	-13.18	5.92	1	0.015
	Rich-club		$\emptyset_{norm}$ ( $k = 18$ )	-77.50	13.26	5.93	1	0.015
			$\emptyset_{norm}$ ( $k = 19$ )	-112.31	19.57	16.36	1	< 0.001
			$\emptyset_{norm}$ ( $k = 20$ )	-81.64	16.45	15.02	1	< 0.001
			$\emptyset_{norm}$ ( $k = 21$ )	-70.26	12.46	5.53	1	0.019

329  $\emptyset_{norm}$ : normalized rich-club coefficient; k: degree; index.  
330 \*Poststroke functional recovery was defined as the changes in functional assessments from baseline.

331 **Table 6.** Summary of prediction models.

Poststroke functional recovery	Model	Variables	AIC	BIC	$\chi^2$	Df	Pr ( $> \chi^2$ )
Change in UE-FM	Baseline	Age, gender, time	192.67	200.88			
	Prediction	Age, gender, time, communication cost ratio of feeder connections, length of rich-club and local connections, $\emptyset_{norm}$ (k = 19)	177.35	191.02	23.33	4	< 0.001
Change in BI	Baseline	Age, gender, time	244.39	252.59			
	Prediction	Age, gender, time, length of local connections, $\emptyset_{norm}$ (k = 18, 19)	228.79	241.09	21.60	2	< 0.001

332  $\emptyset_{norm}$ : normalized rich-club coefficient; k: degree; index.  
333 AIC: Akaike information criterion; BIC: Bayesian information criterion.

## 334 Discussion

335 Our study aims to investigate the relation between poststroke brain functions and functional  
336 recovery versus the rich-club organization of the structural brain network of patient after first-  
337 time acute ischemic stroke. First of all, we investigated the effect of time after stroke on brain  
338 functions, rich-club organization and metrics of the brain network at rich-club and local scales.  
339 Second, we examined the relation between poststroke brain functions versus rich-club  
340 organization and network metrics. Finally, we established models to predict poststroke  
341 functional recovery using the metrics of brain network at rich-club scale and normalized rich-  
342 club coefficient measured at baseline.

## 343 Longitudinal changes in brain network after acute ischemic stroke

344 The rich-club regions that remained unchanged over the course of stroke recovery included the  
345 bilateral dorsolateral superior frontal gyri, right supplementary motor area, and left median  
346 cingulate and paracingulate gyri (**Table 2, Figure 4**). As much as half of the rich-club regions  
347 changed during stroke recovery may suggest that recovery may require remodelling of a  
348 significant portion of rich-club organization. It is noteworthy that the rich-club regions of the  
349 patients at 6 months after stroke, who have largely functionally recovered, were not the same  
350 as those in normal controls as reported by van den Heuvel et al<sup>20</sup>. This discrepancy may suggest  
351 that their networks may be different, although effects due to the difference in postprocessing  
352 could not be ruled out.

353 The properties of the local network of a number of brain regions, majority of which were not  
354 rich-club regions, changed with time after stroke (**Figure 4**). For network connections, the the  
355 density ratio of rich-club connections increased with time after stroke (**Table 3**). Considering  
356 that rich-club regions are highly connected brain regions and density ratio reflects the how  
357 strong the connection is, our results suggest that this increase may be an attempt of the rich-  
358 club organization to further improve communication efficiency to aid poststroke functional  
359 recovery<sup>19</sup>. For feeder and local connections, their density ratio manifested contrasting time  
360 effect, likely suggesting a rebalance of resources, thereby allowing higher communication  
361 capacity for feeder connections that connect rich-club to non-rich-club regions. Schirmer and  
362 Chung showed in a study of the rich-club organization across the life span that the  
363 communication path of feeder connections strengthened, and that of local connections  
364 weakened<sup>43</sup>. Together, these results suggest that rich-club and non-rich-club regions may likely  
365 play very different roles over time.

### 366 **Plausible neuroarchitectural underpinning of poststroke brain functions and functional** 367 **recovery**

368 Our results showed that of all the network properties that correlated with poststroke functions,  
369 communication cost ratio/density ratio of rich-club connections positively correlated with both  
370 motor function and daily activities of daily living (**Table 4**). Considering that the benefit of  
371 rich-club organization is to confer short communication relays to the brain network as a whole,  
372 albeit its high cost of wiring, our results likely suggest that poststroke brain functions may  
373 hinge on the communication efficiency conferred by the rich-club organization<sup>19</sup>.

374

375 For the neuroarchitectural underpinning of poststroke functional recovery (change in  
376 functional assessment from baseline), our results showed that higher normalized rich club  
377 coefficients within a week after stroke were correlated with the recovery of both motor  
378 functions and activities of daily living (**Table 5**), suggesting that residual rich-club  
379 organization of structural brain network after acute stroke may play an important role in  
380 supporting poststroke functional recovery. For the recovery of motor functions, it is interesting  
381 to note that it was correlated with lower density ratio and cost ratio of local connections, higher  
382 density ratio and cost ratio of feeder connections. Our results provide additional support to the  
383 notion that rich-club and non-rich-club regions likely play very different roles not only in  
384 aging<sup>43</sup> but also stroke recovery. For the recovery of activities of daily living, it was negatively

385 correlated with the density, cost and length of local connections, indicating that local  
386 connections may play a more dominant role on the recovery of activities of daily living.

387 Of the baseline network metrics that correlate with poststroke functional recovery, the  
388 communication cost ratio of feeder connections, length of rich-club connections, length of  
389 local connections, and normalized rich-club coefficient could potentially be prognostic  
390 indicators of stroke recovery (**Table 6**). Our findings extended the work by Ktena et al <sup>27</sup> and  
391 Schirmer et al <sup>26</sup> in modelling poststroke functional outcome. Both of their work demonstrated  
392 that the prediction of stroke functional outcome could be improved by the incorporation of the  
393 number of rich-club regions that were affected by stroke.

### 394 **Limitations**

395 Our study still has several limitations. First, the infarct was located in different hemispheres  
396 among the 16 patients. To avoid systematic error, we swapped the brain regions from the two  
397 hemispheres for patients with right-sided infarct to ensure that all infarcts were on the left  
398 hemisphere. However, brain asymmetry may have confounded our results; for example, the  
399 strengths of the left and right hemispheres are not equal<sup>39</sup>. Second, there were some missing  
400 data in our dataset due to patient attrition. We have nonetheless partially circumvented this  
401 problem using data imputation. Finally, we did not have data from control group in order to  
402 investigate the effect of stroke on rich-club organizations, and to compare the difference in  
403 rich-club organization between functionally recovered stroke patients versus healthy controls.  
404

405 **Conclusion**

406 We have successfully demonstrated the relation between poststroke brain functions and  
407 functional recovery versus rich-club organization and network metrics after first-time acute  
408 ischemic stroke. Our results provide additional support to the notion that different types of  
409 network connections play different roles in brain functions as well as functional recovery.

410

## 411 **References**

- 412 (1) Langhorne, P.; Coupar, F.; Pollock, A. Motor Recovery after Stroke: A Systematic  
413 Review. *The Lancet Neurology* **2009**, *8* (8), 741–754.
- 414 (2) Warlow, C. P.; Van Gijn, J.; Dennis, M. S.; Wardlaw, J. M.; Bamford, J. M.; Hankey, G.  
415 J.; Sandercock, P. A.; Rinkel, G.; Langhorne, P.; Sudlow, C. *Stroke: Practical*  
416 *Management*; John Wiley & Sons, 2011.
- 417 (3) Johansson, B. B. Brain Plasticity and Stroke Rehabilitation: The Willis Lecture. *Stroke*  
418 **2000**, *31* (1), 223–230.
- 419 (4) Murphy, T. H.; Corbett, D. Plasticity during Stroke Recovery: From Synapse to  
420 Behaviour. *Nature Reviews Neuroscience* **2009**, *10* (12), 861–872.
- 421 (5) Schaechter, J. D. Motor Rehabilitation and Brain Plasticity after Hemiparetic Stroke.  
422 *Progress in neurobiology* **2004**, *73* (1), 61–72.
- 423 (6) Di Pino, G.; Pellegrino, G.; Assenza, G.; Capone, F.; Ferreri, F.; Formica, D.; Ranieri, F.;  
424 Tombini, M.; Ziemann, U.; Rothwell, J. C. Modulation of Brain Plasticity in Stroke: A  
425 Novel Model for Neurorehabilitation. *Nature Reviews Neurology* **2014**, *10* (10), 597–  
426 608.
- 427 (7) Ward, N. S.; Newton, J. M.; Swayne, O. B.; Lee, L.; Thompson, A. J.; Greenwood, R. J.;  
428 Rothwell, J. C.; Frackowiak, R. S. Motor System Activation after Subcortical Stroke  
429 Depends on Corticospinal System Integrity. *Brain* **2006**, *129* (3), 809–819.
- 430 (8) Kirton, A.; Shroff, M.; Visvanathan, T.; Deveber, G. Quantified Corticospinal Tract  
431 Diffusion Restriction Predicts Neonatal Stroke Outcome. *Stroke* **2007**, *38* (3), 974–  
432 980.
- 433 (9) Stinear, C. M.; Barber, P. A.; Smale, P. R.; Coxon, J. P.; Fleming, M. K.; Byblow, W. D.  
434 Functional Potential in Chronic Stroke Patients Depends on Corticospinal Tract  
435 Integrity. *Brain* **2007**, *130* (1), 170–180.
- 436 (10) Zhu, L. L.; Lindenberg, R.; Alexander, M. P.; Schlaug, G. Lesion Load of the  
437 Corticospinal Tract Predicts Motor Impairment in Chronic Stroke. *Stroke* **2010**, *41* (5),  
438 910–915.
- 439 (11) Newton, J. M.; Ward, N. S.; Parker, G. J.; Deichmann, R.; Alexander, D. C.; Friston, K.  
440 J.; Frackowiak, R. S. Non-Invasive Mapping of Corticofugal Fibres from Multiple  
441 Motor Areas—Relevance to Stroke Recovery. *Brain* **2006**, *129* (7), 1844–1858.
- 442 (12) Lindberg, P. G.; Skejø, P. H.; Rounis, E.; Nagy, Z.; Schmitz, C.; Wernegren, H.; Bring,  
443 A.; Engardt, M.; Forssberg, H.; Borg, J. Wallerian Degeneration of the Corticofugal  
444 Tracts in Chronic Stroke: A Pilot Study Relating Diffusion Tensor Imaging,  
445 Transcranial Magnetic Stimulation, and Hand Function. *Neurorehabilitation and*  
446 *neural repair* **2007**, *21* (6), 551–560.
- 447 (13) Strens, L. H. A.; Asselman, P.; Pogosyan, A.; Loukas, C.; Thompson, A. J.; Brown, P.  
448 Corticocortical Coupling in Chronic Stroke: Its Relevance to Recovery. *Neurology*  
449 **2004**, *63* (3), 475–484.
- 450 (14) Schulz, R.; Braass, H.; Liuzzi, G.; Hoerniss, V.; Lechner, P.; Gerloff, C.; Hummel, F. C.  
451 White Matter Integrity of Premotor–Motor Connections Is Associated with Motor  
452 Output in Chronic Stroke Patients. *NeuroImage: Clinical* **2015**, *7*, 82–86.
- 453 (15) Crofts, J. J.; Higham, D. J.; Bosnell, R.; Jbabdi, S.; Matthews, P. M.; Behrens, T. E. J.;  
454 Johansen-Berg, H. Network Analysis Detects Changes in the Contralateral  
455 Hemisphere Following Stroke. *Neuroimage* **2011**, *54* (1), 161–169.
- 456 (16) McAuley, J. J.; da Fontoura Costa, L.; Caetano, T. S. Rich-Club Phenomenon across  
457 Complex Network Hierarchies. *Applied Physics Letters* **2007**, *91* (8), 084103.
- 458 (17) Harriger, L.; Van Den Heuvel, M. P.; Sporns, O. Rich Club Organization of Macaque  
459 Cerebral Cortex and Its Role in Network Communication. *PloS one* **2012**, *7* (9),  
460 e46497.

- 461 (18) Senden, M.; Deco, G.; De Reus, M. A.; Goebel, R.; Van Den Heuvel, M. P. Rich Club  
462 Organization Supports a Diverse Set of Functional Network Configurations.  
463 *Neuroimage* **2014**, *96*, 174–182.
- 464 (19) van den Heuvel, M. P.; Kahn, R. S.; Goñi, J.; Sporns, O. High-Cost, High-Capacity  
465 Backbone for Global Brain Communication. *Proceedings of the National Academy of*  
466 *Sciences* **2012**, *109* (28), 11372–11377.
- 467 (20) Van Den Heuvel, M. P.; Sporns, O. Rich-Club Organization of the Human Connectome.  
468 *Journal of Neuroscience* **2011**, *31* (44), 15775–15786.
- 469 (21) van den Heuvel, M. P.; Sporns, O.; Collin, G.; Scheewe, T.; Mandl, R. C.; Cahn, W.;  
470 Goñi, J.; Pol, H. E. H.; Kahn, R. S. Abnormal Rich Club Organization and Functional  
471 Brain Dynamics in Schizophrenia. *JAMA psychiatry* **2013**, *70* (8), 783–792.
- 472 (22) McColgan, P.; Seunarine, K. K.; Razi, A.; Cole, J. H.; Gregory, S.; Durr, A.; Roos, R.  
473 A.; Stout, J. C.; Landwehrmeyer, B.; Scahill, R. I. Selective Vulnerability of Rich Club  
474 Brain Regions Is an Organizational Principle of Structural Connectivity Loss in  
475 Huntington’s Disease. *Brain* **2015**, *138* (11), 3327–3344.
- 476 (23) Shu, N.; Duan, Y.; Huang, J.; Ren, Z.; Liu, Z.; Dong, H.; Barkhof, F.; Li, K.; Liu, Y.  
477 Progressive Brain Rich-Club Network Disruption from Clinically Isolated Syndrome  
478 towards Multiple Sclerosis. *NeuroImage: Clinical* **2018**, *19*, 232–239.
- 479 (24) Verhelst, H.; Vander Linden, C.; De Pauw, T.; Vingerhoets, G.; Caeyenberghs, K.  
480 Impaired Rich Club and Increased Local Connectivity in Children with Traumatic  
481 Brain Injury: Local Support for the Rich? *Human brain mapping* **2018**, *39* (7), 2800–  
482 2811.
- 483 (25) Yan, T.; Wang, W.; Yang, L.; Chen, K.; Chen, R.; Han, Y. Rich Club Disturbances of  
484 the Human Connectome from Subjective Cognitive Decline to Alzheimer’s Disease.  
485 *Theranostics* **2018**, *8* (12), 3237.
- 486 (26) Schirmer, M. D.; Ktena, S. I.; Nardin, M. J.; Donahue, K. L.; Giese, A.-K.; Etherton,  
487 M.; Wu, O.; Rost, N. Rich-Club Organization: An Important Determinant of  
488 Functional Outcome after Acute Ischemic Stroke. *Frontiers in neurology* **2019**, *10*,  
489 956.
- 490 (27) Ktena, S. I.; Schirmer, M. D.; Etherton, M. R.; Giese, A.-K.; Tuozzo, C.; Mills, B. B.;  
491 Rueckert, D.; Wu, O.; Rost, N. S. Brain Connectivity Measures Improve Modeling of  
492 Functional Outcome after Acute Ischemic Stroke. *Stroke* **2019**, *50* (10), 2761–2767.
- 493 (28) Sullivan, K. J.; Tilson, J. K.; Cen, S. Y.; Rose, D. K.; Hershberg, J.; Correa, A.;  
494 Gallichio, J.; McLeod, M.; Moore, C.; Wu, S. S. Fugl-Meyer Assessment of  
495 Sensorimotor Function after Stroke: Standardized Training Procedure for Clinical  
496 Practice and Clinical Trials. *Stroke* **2011**, *42* (2), 427–432.
- 497 (29) Kwakkel, G.; Veerbeek, J. M.; Harmeling-van der Wel, B. C.; van Wegen, E.; Kollen,  
498 B. J. Diagnostic Accuracy of the Barthel Index for Measuring Activities of Daily  
499 Living Outcome after Ischemic Hemispheric Stroke: Does Early Poststroke Timing of  
500 Assessment Matter? *Stroke* **2011**, *42* (2), 342–346.
- 501 (30) Andersson, J. L.; Skare, S. A Model-Based Method for Retrospective Correction of  
502 Geometric Distortions in Diffusion-Weighted EPI. *Neuroimage* **2002**, *16* (1), 177–199.
- 503 (31) Talairach, J. 3-Dimensional Proportional System; an Approach to Cerebral Imaging.  
504 Co-Planar Stereotaxic Atlas of the Human Brain. *Thieme* **1988**, 1–122.
- 505 (32) Wang, R.; Benner, T.; Sorensen, A. G.; Wedeen, V. J. Diffusion Toolkit: A Software  
506 Package for Diffusion Imaging Data Processing and Tractography. In *Proc Intl Soc*  
507 *Mag Reson Med*; Berlin, 2007; Vol. 15.
- 508 (33) Mori, S.; Crain, B. J.; Chacko, V. P.; Van Zijl, P. C. Three-Dimensional Tracking of  
509 Axonal Projections in the Brain by Magnetic Resonance Imaging. *Annals of*

- 510 *Neurology: Official Journal of the American Neurological Association and the Child*  
511 *Neurology Society* **1999**, *45* (2), 265–269.
- 512 (34) Mori, S.; Van Zijl, P. C. Fiber Tracking: Principles and Strategies—a Technical Review.  
513 *NMR in Biomedicine: An International Journal Devoted to the Development and*  
514 *Application of Magnetic Resonance In Vivo* **2002**, *15* (7–8), 468–480.
- 515 (35) Rolls, E. T.; Joliot, M.; Tzourio-Mazoyer, N. Implementation of a New Parcellation of  
516 the Orbitofrontal Cortex in the Automated Anatomical Labeling Atlas. *Neuroimage*  
517 **2015**, *122*, 1–5.
- 518 (36) Rubinov, M.; Sporns, O. Complex Network Measures of Brain Connectivity: Uses and  
519 Interpretations. *Neuroimage* **2010**, *52* (3), 1059–1069.
- 520 (37) Colizza, V.; Flammini, A.; Serrano, M. A.; Vespignani, A. Detecting Rich-Club  
521 Ordering in Complex Networks. *Nature physics* **2006**, *2* (2), 110.
- 522 (38) Opsahl, T.; Colizza, V.; Panzarasa, P.; Ramasco, J. J. Prominence and Control: The  
523 Weighted Rich-Club Effect. *Physical review letters* **2008**, *101* (16), 168702.
- 524 (39) Ball, G.; Aljabar, P.; Zebari, S.; Tusor, N.; Arichi, T.; Merchant, N.; Robinson, E. C.;  
525 Ogundipe, E.; Rueckert, D.; Edwards, A. D. Rich-Club Organization of the Newborn  
526 Human Brain. *Proceedings of the National Academy of Sciences* **2014**, *111* (20), 7456–  
527 7461.
- 528 (40) Cnaan, A.; Laird, N. M.; Slasor, P. Using the General Linear Mixed Model to Analyse  
529 Unbalanced Repeated Measures and Longitudinal Data. *Statistics in medicine* **1997**, *16*  
530 (20), 2349–2380.
- 531 (41) Verbeke, G.; Molenberghs, G. *Linear Mixed Models for Longitudinal Data*; Springer  
532 Science & Business Media, 2009.
- 533 (42) Winter, B. Linear Models and Linear Mixed Effects Models in R with Linguistic  
534 Applications. *arXiv preprint arXiv:1308.5499* **2013**.
- 535 (43) Schirmer, M. D.; Chung, A. W. Structural Subnetwork Evolution across the Life-Span:  
536 Rich-Club, Feeder, Seeder. In *International Workshop on Connectomics in*  
537 *Neuroimaging*; Springer, 2018; pp 136–145.
- 538
- 539
- 540
- 541
- 542
- 543
- 544
- 545
- 546
- 547
- 548
- 549
- 550
- 551
- 552
- 553
- 554
- 555
- 556
- 557
- 558